# Clonal origins of relapse in *ETV6-RUNX1* acute lymphoblastic leukemia

Frederik W. van Delft,[1] Sharon Horsley,[1] Sue Colman,[1] Kristina Anderson,[1] Caroline Bateman,[1] Helena Kempski,[2] Jan Zuna,[3] Cornelia Eckert,[4] Vaskar Saha,[5] Lyndal Kearney,[1] Anthony Ford,[1] and Mel Greaves[1]

[1]Section of Haemato-Oncology, Institute of Cancer Research, Sutton, United Kingdom; [2]Paediatric Malignancy Cytogenetics Unit, Great Ormond Street Hospital, London, United Kingdom; [3]CLIP (Childhood Leukaemia Investigation Prague), Department of Paediatric Haematology and Oncology, 2nd Faculty of Medicine, Charles University, Prague, Czech Republic; [4]Department of Pediatric Oncology/Hematology, Charité–Medical University, Berlin, Germany; and [5]CRUK Children's Cancer Group, Manchester Academic Health Sciences Centre, University of Manchester and Central Manchester Hospitals University Trust, Manchester, United Kingdom

**B-cell precursor childhood acute lymphoblastic leukemia with *ETV6-RUNX1* (*TEL-AML1*) fusion has an overall good prognosis, but relapses occur, usually after cessation of treatment and occasionally many years later. We have investigated the clonal origins of relapse by comparing the profiles of genomewide copy number alterations at presentation in 21 patients with those in matched relapse (12-119 months). We identified, in total, 159 copy number alterations at presentation and 231 at relapse (excluding Ig/TCR). Deletions of *CDKN2A/B* or *CCNC* (6q16.2-3) or both increased from 38% at presentation to 76% in relapse, suggesting that cell-cycle deregulation contributed to emergence of relapse. A novel observation was recurrent gain of chromosome 16 (2 patients at presentation, 4 at relapse) and deletion of plasmocytoma variant translocation 1 in 3 patients. The data indicate that, irrespective of time to relapse, the relapse clone was derived from either a major or minor clone at presentation. Backtracking analysis by FISH identified a minor subclone at diagnosis whose genotype matched that observed in relapse ~ 10 years later. These data indicate subclonal diversity at diagnosis, providing a variable basis for intraclonal origins of relapse and extended periods (years) of dormancy, possibly by quiescence, for stem cells in *ETV6-RUNX1*$^+$ acute lymphoblastic leukemia. (*Blood*. 2011;117(23):6247-6254)**

## Introduction

The translocation t(12;21)(p13;q22) generating *ETV6-RUNX1* (*TEL-AML1*) gene fusion is a consistent genetic abnormality in 25% of childhood B-cell precursor acute lymphoblastic leukemia (ALL).[1] It typically occurs in young patients and is only occasionally detected in adolescents and young adults.[2] Guthrie card analysis and twin studies have previously shown that the *ETV6-RUNX1* fusion gene frequently originates before birth, probably as an initiating lesion.[3-5] Preleukemic clones with *ETV6-RUNX1* are generated prenatally at a rate considerably in excess of clinical ALL.[6] This, plus the modest concordance of ALL in monozygotic twins (10%-15%), suggests that additional, postnatal mutations are necessary for progression to overt malignancy.[4] Modeling studies with both murine[7] or human[8] cells support this contention. Cytogenetic analyses have identified secondary chromosomal abnormalities associated with *ETV6-RUNX1*$^+$ ALL of which deletion of the non-rearranged *ETV6* allele appears the most frequent (~ 70%).[9] This ALL subtype generally has a favorable prognosis.[10] Relapses when they do occur are usually in patients off treatment.[11] These may occur several years after cessation of treatment[12-14] and occasionally after 10-20 years.[15] Clonotypic Ig/TCR markers indicate that very late relapsing ALLs are clonally derived from the initially presenting clones.[16] A striking feature of late relapsing cases of ALL is that they are chemosensitive with durable term remissions possible.[17,18] This implies that their initial survival and reemergence is related to properties other then mutation-based drug resistance. Comparison of the genomic boundaries (by microsatellite markers) of *ETV6* deletions at diagnosis and relapse has previously shown that these differ in some but not all cases.[19,20] One plausible interpretation of this finding is that the relapse clone can derive from a minor clone present at diagnosis. This view is endorsed by IgH clonotypic markers in which the dominant rearrangement observed at relapse is detectable by PCR as a minor clone at diagnosis.[13,19-23] The nature of such minor clones is unclear from such studies, but one suggestion was that they might represent persistent preleukemic stem cells[8] with *ETV6-RUNX1* but lacking both *ETV6* deletion and all other secondary genetic changes.[19,20]

Recent developments in whole genome scanning provide a greater depth of interrogation of clonal relationships. Genomic analyses with the use of high-density single nucleotide polymorphism (SNP) arrays have recently shown an average of ~ 6 chromosomal copy number alterations (CNAs) in childhood ALL with *ETV6-RUNX1* fusion gene.[21] Three recent studies have used high-density CNA analysis to try and elucidate the molecular mechanism of disease recurrence in childhood ALL. These 3 studies have shown an increase in CNAs between presentation and relapse, with B-cell development and cell-cycle regulation pathways most often affected.[22,24,25] In most cases the presenting and relapse clones contained some identical CNAs, suggesting a shared clonal origin. This was confirmed by back-tracking PCR some of the genetic lesions originally identified at relapse by SNP analysis. In most cases the relapse "specific" lesion was present at low level at presentation in a minor subclone.[22] The investigators of that study equated minor subclones to ancestral clones in a linear clonal

Submitted October 22, 2010; accepted March 15, 2011. Prepublished online as *Blood* First Edition paper, April 11, 2011; DOI 10.1182/blood-2010-10-314674.

The online version of this article contains a data supplement.

The publication costs of this article were defrayed in part by page charge payment. Therefore, and solely to indicate this fact, this article is hereby marked "advertisement" in accordance with 18 USC section 1734.

succession model.[22] If, as speculated previously, some very late relapses in ALL derive from preleukemic clones, then these relapses should have a distinct profile of CNAs absent at diagnosis, and no individual relapse CNAs should be identifiable at diagnosis. We acquired a series of matched presentation/remission/relapse DNA samples from 21 pediatric patients with *ETV6-RUNX1*$^+$ ALL who had relapses of various time intervals from initial diagnosis to evaluate clonal origins of relapse. The described origin of relapse analysis was performed with the caveat that complete genomic characterization of the cell of origin remains elusive at present. *ETV6-RUNX1* itself, we presumed, should provide, as the probable initiating lesion, a stable marker of all descendent clones along with $\geq 1$ clonotypic Ig or TCR rearrangements.[4,20]

## Methods

### Patients

Twenty-one patients with relapsed *ETV6-RUNX1*–positive childhood ALL were studied (see supplemental Table 1 for patient characteristics, available on the *Blood* Web site; see the Supplemental Materials link at the top of the online article). The samples were obtained from the Academic Department of Paediatric Oncology, The Royal London Hospital, United Kingdom, Great Ormond Street Hospital, United Kingdom, Department of Pediatric Oncology/Hematology, Charité–Medical University, Berlin, Germany, and Childhood Leukemia Investigation Prague, Department of Paediatric Hematology and Oncology, 2nd Faculty of Medicine, Charles University Prague, Czech Republic. The ethics committee or institutional review board of each participating center approved the study. Informed consent was obtained from all subjects in accordance with the Declaration of Helsinki. The diagnosis of *ETV6-RUNX1* ALL was established through FISH and PCR analysis as per local protocols. Samples were selected on the basis of availability of DNA or viable cells at initial presentation, remission, and relapse (R) with blast purity of $\geq 75\%$ before extraction of DNA. The median age at diagnosis was 4.5 years (range, 1.93-15.8 years). Time to first relapse from diagnosis was $< 2$ years (ie, on treatment) to 9 years 11 months. Five of 14 patients with data available had a white cell count $> 20 \times 10^9$/L. At initial presentation the BM was the only site involved in all patients, whereas at relapse the BM was involved in isolation in 15 patients, combined BM and testis in 3 patients, CNS was involved in 2 relapses, and in 1 patient the data were not available. The patients were treated on a variety of protocols, namely UK ALL X/XI, 97/01, 2003, UKALL R2, BFM 90, 95, 2000, 2002, COALL 92, 97, 2003. At submission of this document 9 patients were in complete remission after first or second relapse. Ten patients died after second relapse. The outcome of 2 patients remains unknown. In 21 patients adequate matched presentation and relapse DNA were available for genomewide CNA and loss of heterozygosity (LOH) investigations. Matched remission DNA was available for all but unique patient number (UPN) 2.

### Genome mapping analysis

Mapping analysis was performed with 500 ng of tumor and germline DNA from each patient. DNA was prepared according to the manufacturer's instructions with the use of the GeneChip mapping 500K assay protocol for hybridization to GeneChip Mapping 250K Nsp and Sty arrays (Affymetrix). Briefly, genomic DNA was digested in parallel with restriction endonucleases *Nsp*I and *Sty*I, ligated to an adaptor, and subjected to PCR amplification with adaptor-specific primers. The PCR products were digested with *DNase*I and labeled with a biotinylated nucleotide analog. The labeled DNA fragments were hybridized to the microarray, stained by streptavidin-phycoerythrin conjugates, washed with the Affymetrix Fluidics Station 450, and then scanned with a GeneChip scanner 3000 7G. The CEL files are available for download on http://www.icr.ac.uk/array/array.html.

### Copy number and LOH analysis

SNP genotypes were obtained with the use of Affymetrix GCOS software (Version 1.4) to obtain raw feature intensity and Affymetrix GTYPE software (Version 4.0) with the use of the BRLMM to derive SNP genotypes (see supplemental Table 2 for the 250K Sty/Nsp call rates). Samples were analyzed with CNAG 3.0 (http://plaza.umin.ac.jp/genome/) with the use of paired tumor (test) samples with the self-reference control (reference) samples to determine copy number and LOH caused by imbalance.[26] The position of regions of LOH and gain were identified with the University of California Santa Cruz Genome Browser (May 2004 Assembly; http://genome.ucsc.edu/cgi-bin/hgGateway). All samples were also analyzed with dChip (May 2008; www.dchip.org) to verify findings obtained with CNAG.[27,28] The remission samples were assigned a copy number of 2 and were used as a reference set to calculate copy number in tumor samples. Median smoothing with a window size of 5 was used to infer copy number along each chromosome. LOH analysis was done with dChip with the use of a Hidden Markov Model to infer the probability of LOH on the basis of the paired control/tumor samples, using an average heterozygosity rate of 0.33.

### Quantitative genomic PCR

The genomic copy number of the gene *CDKN2A* was confirmed with Taqman Real-Time PCR (RQ-PCR). The Taqman probe and primers were designed with Primer Express Version 3.0 (Applied Biosystems). The Taqman probes were labeled with FAM (5′) and BHQ-1 (3′). The PCR reactions were performed in triplicate on the ABI 7900 PCR machine (Applied Biosystems) as per the manufacturer's protocol. The primer sequence used was *CDKN2A* F, 5′-GACTGCGGAGCAATGAAGACT-3′; *CDKN2A* R, 5′-GATGCAACTGGCCCTAGTTTG-3′; and probe, *CDKN2A* 5′-TAGAGGTCTAGTGCCCC-3′. The gene copy number was measured by Relative Quantification assay with the use of *RNAseP* (Applied Biosystems) as amplification control. The gene copy number was measured in presentation, relapse, and matched remission (germline) DNA. Data evaluation was performed with the ABI 7500 SDS software. A fold change ratio of target gene/housekeeping gene $< 0.7$ was considered indicative of gene deletion (see supplemental Table 3 for the results of the genomic RQ-PCR).

### Fluorescence in situ hybridization

Fixed cytospins were prepared from archival viable cells from UPN2 and UPN19. Interphase FISH for the *ETV6-RUNX1* fusion gene was performed with a commercial LSI *TEL-AML1* extra signal (ES) probe (Vysis; Abbott Laboratories Ltd), according to the manufacturer's instructions. This probe set contains a 350-kb probe for the 5′ end of *ETV6* (exons 1-4) and a 500-kb probe covering the entire *RUNX1* gene. The FISH signal pattern for *ETV6-RUNX1* fusion gene–positive cells with the use of the Vysis probe is 2 red (1 large, 1 small *RUNX1* signal), 1 green (*ETV6* allele not involved in the translocation), 1 red/green (yellow) fusion signal corresponding to the *ETV6-RUNX1* fusion gene. Fosmid probes for *PAX5* (Fosmid G248P800846D3) and *CDKN2A/CDKN2B* (Fosmid G248P882010F5) were obtained from the BACPAC Resource Center, Children's Hospital, Oakland Research Institute (http://bacpac.chori.org). These were labeled by nick translation with biotin-16-dUTP (Roche Diagnostics) as previously described[29] and hybridized in combination with the *ETV6-RUNX1* ES probe. Hybridization and washes were performed according to the Vysis protocol, with a single layer of cyanine 5–conjugated streptavidin (GE Healthcare) for detection of biotinylated fosmids. Fluorescent signals were viewed with a Zeiss Axioskop fluorescence microscope equipped with filters for DAPI (4′-6′-diamidine-2-phenylindole), FITC/Spectrum Green, Spectrum Orange, and cyanine 5. Images were captured and analyzed with a Hamamatsu ORCA-ER CCD camera and SmartCapture X software (Digital Scientific).

### Cloning and backtracking of *ETV6-RUNX1* genomic breakpoint fusion sequence

Amplification of the genomic breakpoint fusion sequences for *ETV6-RUNX1* at relapse was performed by long-range PCR with the use of

**Table 1. Frequency of DNA CNAs in diagnosis and relapsed *ETV6-RUNX1* ALL**

| | Presentation, mean CNA (range) | | Relapse, mean CNA (range) | |
|---|---|---|---|---|
| | All CNA | Driver CNA | All CNA | Driver CNA |
| Deletions | 6.62 (0-16) | 3.05 (0-6) | 9.10 (0-19) | 4.05 (0-8) |
| Gains | 0.95 (0-6) | 0.71 (0-5) | 1.90 (0-6) | 0.81 (0-4) |
| Total CNAs | 7.57 (0-17) | 3.76 (0-9) | 11.0 (0-21) | 4.86 (0-10) |

CNAs in TCR or Ig loci or both are not included in this table.

conditions and primers previously described.[30] The breakpoint sequence was obtained through restriction analysis by primer walking and sequencing (supplemental Figure 8). Patient-specific primers for amplification of fusion breakpoints were designed so that PCR yielded a product of 130-300 bp. DNA from presentation material was then amplified with these primers, and resulting products were sequenced to confirm identity with *ETV6-RUNX1* intronic fusion in relapse samples (UPN15). In 2 cases (UPN14 and UPN19) backtracking analysis was performed with the sequence of the fusion gene isolated at relapse. For each patient fusion breakpoint specific primers and real-time probe were designed. A dilutional series was made with DNA from relapse diagnosis and DNA pooled from mononuclear cells from 10 healthy volunteers. Genomic real-time quantitative PCR was used to identify and quantify the presence of the fusion sequence at diagnosis (data not shown).

## Results

### Recurrent CNAs in *ETV6-RUNX1*–positive ALL

We performed genomewide analysis of CNAs and LOH on matched diagnostic and relapse BM samples from 21 pediatric patients with precursor B-cell ALL carrying an *ETV6-RUNX1* fusion gene [t(12;21)(p12;q22)] (see supplemental Table 1 for patient characteristics). DNA copy number and LOH were obtained with the use of the Affymetrix 500K arrays. These arrays interrogate ~ 500 000 loci. The average distance between SNPs is 5.8 kb.

A total of 159 CNAs at diagnosis and 231 at relapse were identified (excluding physiologic CNAs at the *TCR* and/or *Ig* loci) with a mean of 7.57 CNAs per sample (range, 0-17 CNAs per sample) at initial presentation (Table 1; see supplemental Table 4 for a detailed overview of all CNAs detected). Deletions outnumbered gains by ~ 6.95:1. Eighteen recurrent alterations were found in ≥ 2 diagnostic samples in this series. The most frequently recurring alterations at presentation were deletion of *ETV6* (n = 15), *CDKN2A* (n = 4), *CDKN2B* (n = 3), 6q16.2-3 (n = 4), *FHIT* (n = 4), and *IL3RA/CSF2RA* (n = 5). The most frequently gained regions were 21q22.11-q22.12 (n = 5), Xq26.2-q28 (n = 5), and 12p13.33-p13.31 (n = 2). At diagnosis, 48% of samples showed ≥ 1 deletions in B-cell development regulators; *FHIT* (n = 4), *BTG* (n = 3), *RAG1/2* (n = 2), *CD200/BTLA* (n = 2), *EBF1* (n = 2), *PAX5* (n = 2), *IKZF1* (n = 1), and *TCF3* (n = 1).

**Table 2. Most frequently targeted genes and gene regions at presentation and relapse in *ETV6-RUNX1* ALL**

| Lesion | Gene | Presentation | Relapse |
|---|---|---|---|
| Deletion | *ETV6* | 15 | 14 |
| | *CDKN2A* | 4 | 9 |
| | *CDKN2B* | 3 | 6 |
| | 6q16.2-3 | 4 | 7 |
| | *BTG* | 3 | 6 |
| | *IL3RA/CSF2RA* | 5 | 5 |
| | *TBL1XR1* | 2 | 3 |
| | *FHIT* | 4 | 3 |
| | *TOX* | 3 | 1 |
| | *RAG1/2* | 2 | 2 |
| | *CD200/BTLA* | 2 | 3 |
| | *DMD* | 1 | 3 |
| | *EBF* | 2 | 3 |
| | 13q14.2-3 | 1 | 3 |
| | *PAX5* | 2 | 4 |
| | MKKS/ORF94 | 1 | 3 |
| Gain | 21q22.11-22.12 | 5 | 7 |
| | Xq26.2-28 | 5 | 2 |
| | 16 | 2 | 4 |
| | 12p13.33-13.31 | 2 | 2 |

These CNAs occurred in ≥ 4 samples.

Next we classified gene alterations as probable "driver" or "passenger" mutations. We defined driver mutations as genes that are mutated on a recurrent basis in leukemia or are probably involved in leukemogenesis or both. Passenger mutations are defined as nonrecurrent or have no known or predicted role in leukemogenesis at present or both. The caveat of this approach is the potentially incorrect labeling of drivers as passengers because of the lack of functional studies. Of the 7.36 (mean) CNAs detected at presentation, 3.76 were classified as potential drivers on the basis of recurrence in this or prior series of cases[21,22,31-33] (Table 1).

At relapse the mean number of CNAs per sample increased to 11.0 (range, 0-21), 4.86 being potential drivers (Table 1). No new recurrent genomic alterations were identified compared with diagnosis, but the frequency of particular CNAs changed, as shown in Table 2. At relapse 57% of samples showed deletions in B-cell development regulator genes.

Next, we compared the evolution of individual gene CNAs between presentation and relapse within each patient. Three patterns were established: (1) CNAs at presentation were lost at relapse, (2) new alterations were gained at relapse, or (3) an alteration persisted from presentation to relapse. More detailed analysis of driver mutation evolution identifies a change in the pattern of driver mutations between presentation and relapse in most patients. In the 21 presentation samples a total of 20 copy number gains were detected. Twelve (60%) of these genomic gains persisted in the relapse samples (Table 3). Of the 139 copy number losses at presentation, 98 (71%) remained detectable at relapse. Overall, of 52 driver mutations persisting between presentation and relapse, 49 (94.2%) had identical chromosomal breakpoints at both time points, with the level of resolution determined by 500K SNP array analysis. In 14 patients ≥ 1 identical copy number change in a driver mutation were present at both presentation and relapse (see supplemental Table 5 for evolution of driver mutations present at presentation and relapse). Of the remaining 7 patients, 6 (UPN6, UPN7, UPN11, UPN14, UPN25, and UPN27) shared ≥ 1 TCR or Ig rearrangement or both (confirmed by PCR and sequencing for UPN6 and UPN11) between presentation and relapse. No rearrangement data were available for 1 patient (UPN19) at initial presentation, but for this patient we have demonstrated identical fusion breakpoint sequences at presentation and relapse (see supplemental Table 6 for Ig and TCR rearrangement analyses at presentation and relapse; supplemental Figure 8 for genomic breakpoint sequences). In 16 of 21 relapsed patients a total of 9 new copy number gains and 41 deletions in driver loci appeared at relapse. At relapse the newly acquired gains were distributed on 4 chromosomal regions, namely 21q22.1-22.12 (including *RUNX1*; n = 3), part or whole of chromosome 16 (n = 3), Xq26.2-28 (n = 2), and 10p (n = 1). The gene loci newly deleted at relapse were *CDKN2A/B* (n = 7;

**Table 3. Total number of CNAs identified at presentation and relapse in *ETV6-RUNX1* ALL**

| | Gains | | | Losses | | | | |
|---|---|---|---|---|---|---|---|---|
| ID | Diagnosis | Relapse | Shared | Diagnosis | Relapse | Shared | Age at presentation, y | Remission duration, mo |
| 2 | 2 | 3 | 2 | 9 | 16 | 8 | 3.92 | 119 |
| 6 | 1 | 3 | 0 | 1 | 15 | 1 | 4.82 | 51 |
| 7 | 0 | 0 | 0 | 7 | 1 | 0 | 5.48 | 34 |
| 8 | 1 | 3 | 1 | 3 | 4 | 0 | 1.93 | 24 |
| 9 | 1 | 1 | 1 | 6 | 7 | 6 | 3.91 | 12 |
| 10 | 0 | 6 | 0 | 7 | 15 | 5 | 5.16 | 36 |
| 11 | 1 | 2 | 0 | 1 | 9 | 1 | 4.50 | 42 |
| 13 | 0 | 0 | 0 | 2 | 4 | 2 | 4.5 | 66 |
| 14 | 1 | 1 | 1 | 12 | 0 | 0 | 7.2 | 33 |
| 15 | 1 | 4 | 0 | 16 | 14 | 13 | 5.5 | 19 |
| 16 | 1 | 2 | 0 | 16 | 19 | 16 | 4.3 | 35 |
| 17 | 2 | 4 | 1 | 10 | 13 | 4 | 3.5 | 76 |
| 18 | 6 | 5 | 5 | 7 | 8 | 6 | 5.8 | 61 |
| 19 | 2 | 1 | 0 | 3 | 9 | 0 | 4.2 | 90 |
| 20 | 0 | 0 | 0 | 13 | 15 | 13 | 15.8 | 22 |
| 21 | 0 | 1 | 0 | 3 | 6 | 3 | 4.1 | 32 |
| 22 | 0 | 0 | 0 | 9 | 16 | 9 | 1.1 | 44 |
| 23 | 1 | 1 | 1 | 3 | 4 | 3 | 2.8 | 37 |
| 25 | 0 | 3 | 0 | 0 | 6 | 0 | 8.7 | 54 |
| 26 | 0 | 0 | 0 | 8 | 10 | 8 | 6.7 | 30 |
| 27 | 0 | 0 | 0 | 3 | 0 | 0 | 1.9 | 22 |
| Total | 20 | 40 | 12 | 139 | 191 | 98 | | |

Shared CNAs are present at presentation and relapse in the same patient. CNAs in TCR or Ig loci or both are not included in this table.

hemizygous, n = 5; homozygous, n = 2), 6q16.2-3 (n = 4), *ETV6* (n = 3), *BTG1* (n = 3), *DMD* (n = 3), *EBF1* (n = 2), *RB1* (n = 2), 13q14.2-3 (n = 2), *MKKS/ORF94* (n = 2), *PAX5* (n = 3), *LTK* (n = 2), *DPF3* (n = 2), *ELF1* (n = 1), *CD200/BTLA* (n = 1), *PVT1* (n = 1), *HIST* (n = 1), *IL3RA/CSF2RA* (n = 1), and *TBL1XR1* (n = 1). No new driver mutations were observed at relapse in 5 patients (UPN7, UPN9, UPN13, UPN14, and UPN27). Analysis with dChip for frequent CNAs on chromosome 12p (*ETV6*), 9p (*CDKN2A*), and 6q16.2-3 is shown in Figure 1A, B, and C, respectively. The region of deletion on 6q varied in size between the samples. The minimally deleted region was located on 6q16.1-22.1 (95 699 306-115 623 936 bp) containing 72 well-characterized genes and 9 open reading frames, including *CCNC*, *GRIK2*, and *ARMC2* and 1 microRNA coding region (miR-587).

Two patients in this cohort had 2 consecutive relapses each. Patient UPN6 relapsed after 51 (6R1, BM) and 77 (6R2, isolated testes) months, and patient UPN10 after 36 (10R1, BM) and 80 (10R2, BM) months since initial presentation. In the first patient the only driver mutation shared between initial presentation and both relapses was the *ETV6-RUNX1* fusion gene. Analysis of TCR and Ig rearrangements by SNP and RQ-PCR/sequencing showed shared clonal origins. Thirteen driver CNAs were shared between R1 and R2. Between R1 and R2 deletion of 6p25.3-25.2 and gain of 16p13.3-12.3 were lost, and deletion of 12p13.2 (*ETV6*) appeared. In the latter patient, 5 driver mutations were shared between the presenting and relapse clones, and R1 and R2 shared 18 CNAs. At R2 the clone additionally acquired deletion 8q24.21 (*PVT1*) in comparison with R1. Deletion of 8q12.1 (*TOX*) was present at presentation and again at second relapse R2. Gain of the short arm of chromosome 16 at R1 was lost at second relapse R2.

### Clonal origins of relapse versus time of relapse

Mullighan et al[22] and Kuster et al[25] used a relapse classification, based on comparative CNA profiles which distinguished clonal origins as either from the "diagnostic" (ie, major) clone or an "ancestral" (ie, precursor and minor) clone present at presentation. Although this is a pragmatic scheme, it makes implicit assumptions about subclonal heterogeneity and ancestral relationships at presentation which are currently uncertain. We therefore selected to use a modified scheme. (Table 4) This classifies relapses into 4 CNA profiles, and for each of these we indicate possible clonal origins with respect to the matched presentation sample. This classification is purely based on driver mutation alterations as detected by the 500K SNP array analysis. In addition, it assumes the persistence of an identical *ETV6-RUNX1* fusion gene at presentation and relapse in all cases, as previously shown with matched presentation/relapse samples.[20] In our current cohort we confirmed identity of *ETV6-RUNX1* genomic sequence in 3 paired diagnostic/relapse samples (UPN14, UPN15, and UPN19; supplemental Figure 8). We distinguished the following 4 profiles: (type 1) the relapse clone resembles the initially presenting leukemia clone, (type 2) the relapse clone has acquired extra driver mutation(s), (type 3) the relapse clone showed losses and gains of driver mutations, and (type 4) the relapse clone has lost all CNAs present initially and acquired a completely new set of alterations. Any samples not fitting these descriptions were defined as unclassified. Of the 21 matched presentation relapse patient samples, 2 patients were classified as type 1 (UPN9 and UPN13), 7 patients were type 2 (UPN2, UPN10, UPN20, UPN21, UPN22, UPN23, and UPN26), 6 as type 3 (UPN8, UPN11, UPN15, UPN16, UPN17, and UPN18), and 4 as type 4 (UPN6, UPN7, UPN14, and UPN19). Two patients were defined as unclassified (UPN25 and UPN 27).

Next, we considered the duration of remission in each of the classified patients and sought a potential relationship between remission duration and the clonal origin of relapse, with the realization that our patients received different therapies and that outcome for ALL is protocol driven, potentially clouding interpretation of data. We used the following time cutoffs: very early relapse $< 2$ years, early relapse 2-5 years, and late relapse $> 5$ years since initial presentation. A random distribution of relapse types 1-4 was observed in the very early, early, and late relapse

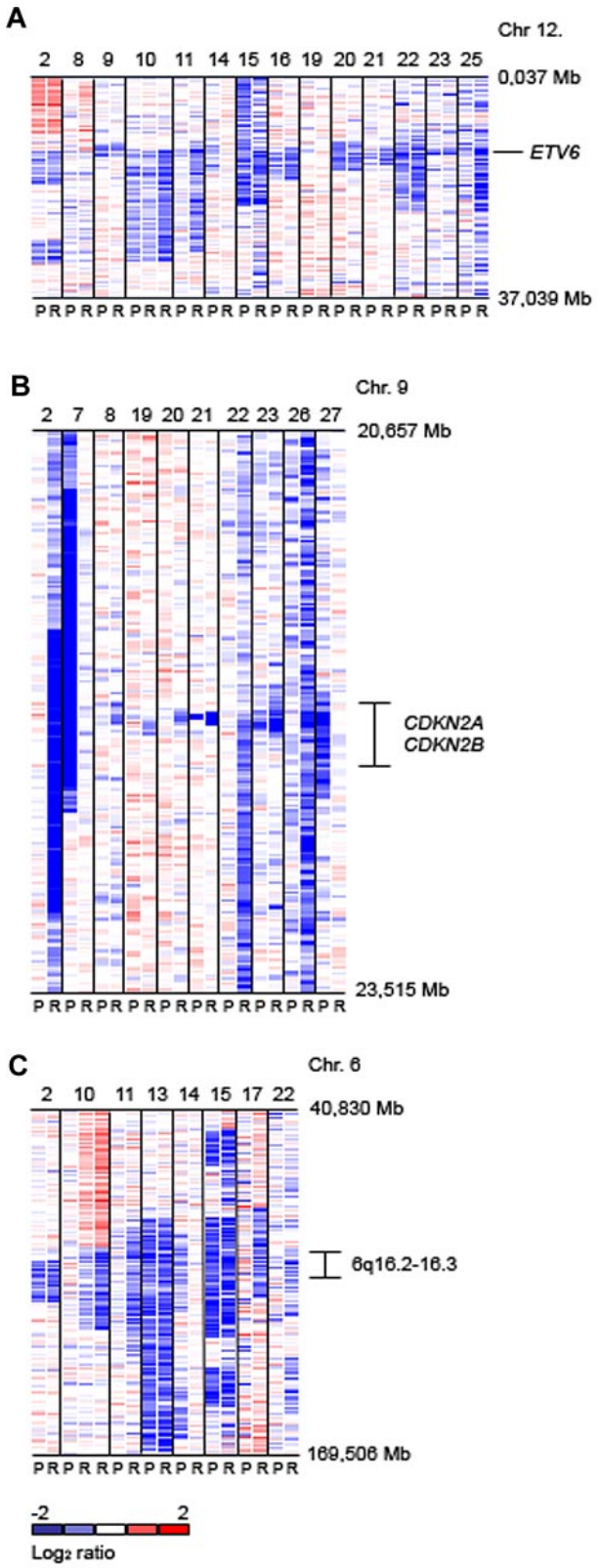


**Figure 1. $Log_2$ ratio SNP 500K copy number data (median smoothed with a window of 5 markers; blue is loss and red is gain).** (A) Genomic copy number of chromosome 12p flanking *ETV6* for 14 representative cases showing deletions at this locus at presentation (P) and relapse (R). (B) Copy number of chromosome 9p flanking *CDKN2A/B*. (C) Copy number of chromosome 6q. The chromosomal region of 6q16.2-3 which is recurrently deleted in pediatric ALL is indicated.

categories, as shown in Table 4, without a clear increase in type 3 or 4 in case the remission duration was $\geq 5$ years. We also observed no correlation between total number of driver mutations at relapse and the length of remission. When we compared the number of newly acquired driver mutations at relapse in function of the length of remission duration, we observed an increase in the average number of new drivers with an increase in remission duration ($< 2$ years: average of 0.75 new drivers; 2-5 years: average of 2.5 new drivers; $> 5$ years: average of 3.0 new drivers); however, this difference was not significant. The total number of driver mutations or newly acquired driver mutations at relapse did not correlate with survival. In our cohort, the type of relapse did correlate with survival. All patients with type 4 relapses (4 of 4) remain in complete continuous remission (median follow-up, 8.9 years; range, 4.7-10.2 years), whereas only 5 of 15 patients with a type 1-3 relapse are alive and in continuous remission (median follow-up, 6.1 years; range, 3.2-10.2 years; supplemental Table 1).

### Backtracking of relapse clone to original presentation

In our series, patient UPN2 experienced the longest remission duration, namely 9 years 11 months. To establish whether in this case the relapse clone was present as a minor subclone at initial presentation, we used FISH to detect relapse clone specific CNAs in the presentation sample. The SNP array data suggested duplication of the *ETV6-RUNX1* fusion gene and loss of wild-type *ETV6* at presentation and relapse and hemizygous loss of 9p (including *CDKN2A* and *PAX5*) in addition to loss of the other *CDKN2A* allele (homozygous loss of *CDKN2A*) at relapse (supplemental Table 4). FISH analysis of the presentation and relapse samples was performed in 702 and 582 cells, respectively (supplemental Table 7). The FISH analysis of the presentation sample confirmed the presence of a dominant leukemic clone with duplication of the fusion gene and loss of the nontranslocated *ETV6* in 72.4% of cells. These cells did not show deletion of *CDKN2A*. Hemizygous loss of *CDKN2A* occurred in 21.3% of cells. A small clone (0.4%) was detected with a genotype identical to the relapse clone, with duplication of the fusion gene, loss of wild-type *ETV6*, and homozygous loss of *CDKN2A* (Figure 2). At relapse, most cells showed duplication of the fusion gene, loss of the nontranslocated *ETV6*, and homozygous loss of *CDKN2A* (79.8%). Leukemic cells with no or hemizygous loss of *CDKN2A* were visualized in 11.5% and 1.4%, respectively (supplemental Figures 4,6). *CDKN2A* deletion-specific backtracking PCR was unsuccessful in this patient. Parallel FISH analysis at presentation and relapse with probes for *ETV6*, *RUNX1*, and *PAX5* was performed and confirmed the genotype of the dominant clones at both time points, that is, duplication of the fusion gene and 2 copies of *PAX5* in 89.14% of cells at presentation and duplication of the fusion gene and 1 copy of *PAX5* in 60.4% of cells (supplemental Table 7; supplemental Figures 5-6).

The SNP array analysis has identified duplication of the *ETV6-RUNX1* fusion gene and loss of wild-type *ETV6* at presentation and relapse and hemizygous loss of 9p (including *CDKN2A* and *PAX5*) in addition to loss of the other *CDKN2A* allele (homozygous loss of *CDKN2A*) at relapse (supplemental Table 4). The homozygous loss of *CDKN2A* and hemizygous loss of *PAX5* in the relapse clone could have arisen in several different ways. The FISH analysis at presentation and relapse with the use of using *ETV6, RUNX1, CDKN2A* or *ETV6, RUNX1,* and *PAX5* probes suggested focal loss of *CDKN2A* before loss of the unaffected chromosome 9p containing *CDKN2A* and *PAX5* (supplemental Table 7; supplemental Figure 7).

**Table 4. Classification of clonal origin in relapsed *ETV6-RUNX1* ALL**

| Presentation | Relapse | Possible clonal origins of relapse | Patient* remission duration, y | | |
|---|---|---|---|---|---|
| | | | < 2 | 2-5 | > 5 |
| Type 1 | ABC → ABC | Dominant clone at diagnosis† | 9 | | 13 |
| Type 2 | ABC → ABC + DE | Dominant clone at diagnosis with further CNA or derivative‡ | 20 | 10,26 | 2 |
| | | minor clone selected with or without further CNA | | | |
| | | | | 21 | |
| | | | | 22 | |
| | | | | 23 | |
| Type 3 | ABC → AB + DE | Minor clone at diagnosis selected with or without further CNA | 8 | 11 | 17 |
| | | | 15 | 16 | 18 |
| Type 4 | ABC → DEF | Minor clone at diagnosis selected either | | 6 | 19 |
| | | (1) Preleukemia/ancestral with all CNAs gained | | 7 | |
| | | (2) Leukemic clone with or without further CNAs | | 14 | |

Type 1-4 describe the observed evolution of driver mutations as defined by the SNP array profile. ABCDEF are driver-only CNAs. In addition to the presence of these driver mutations, this model presumes the persistence of the *ETV6-RUNX1* fusion gene. Each of the relapsed patients (UPN2-UPN27) is classified on the basis of driver CNA evolution between presentation and relapse (type 1-4) and duration of remission since initial diagnosis.

*Unique patient numbers given.

†But other cryptic mutations may be present indicative of evolution.

‡Derived from major or dominant clone at diagnosis.

## Discussion

The patterns of CNAs we observed at diagnosis and relapse of *ETV6-RUNX1*–positive ALL parallel those reported in previous studies of unselected ALL. Overall, there was an increase in the number of CNAs per case in relapses.[22,24,25,31] The genes or regions predominantly involved were also as previously described with the 2 most frequently implicated pathways being cell-cycle regulation and B-cell development.[21,22,24,31-33] In agreement with a recent study,[34] we identified frequent gain of part or whole of chromosome 16 (supplemental Figure 1). This finding has occasionally been described in hematologic malignancy but its significance is unclear. Another novel observation was the deletion of plasmacytoma variant translocation 1 (*PVT1*) at 8q24 in 3 cases (supplemental Figure 2). The significance of deletion of *PVT1* in our cohort remains unclear. *Pvt1* is a nonprotein coding gene located 3′ of myc, and this locus harbors several miRNAs. Hsa-miR-1204 is often fused to the immunoglobulin light chain in variant Burkitt lymphoma and present in *MYC/PVT1* coamplified tumors.[35] Coamplification of *MYC* and *PVT1* has also been identified in human astrocytomas,[36] in breast and ovarian cancers,[37] and in acute myeloid leukemias and myelodysplastic syndromes.[38]

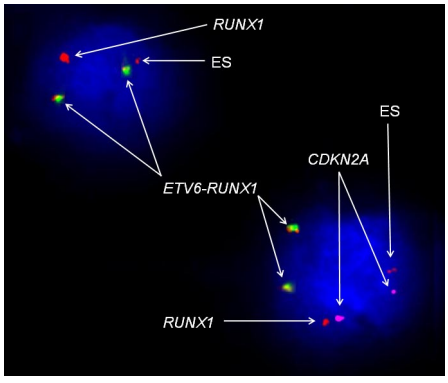


**Figure 2. FISH analysis of UPN2 at presentation, using the LSI *TEL/AML1* ES Dual-Color translocation probe (Vysis) and *CDKN2A* probe.** The red signal represents the *RUNX1* probe; green, the *ETV6* probe; yellow, the *ETV6-RUNX1* fusion gene; and purple, the *CDKN2A* probe. This image represents 2 different leukemic cells at presentation. The cell in the right bottom corner represents the dominant leukemic clone (according to the SNP array data analysis), with duplicated fusion gene, loss of wild-type *ETV6*, 2 copies of *CDKN2A*, 1 normal *RUNX1*, and 1 ES (72% of total cells analyzed). In the left top corner FISH analysis identified a leukemic cell with a constellation of signals corresponding to the dominant relapse clone, that is, a duplicated fusion gene, loss of wild-type *ETV6*, 1 normal *RUNX1*, 1 ES, and complete loss of *CDKN2A* (0.4% of total cells analyzed). In control experiments with normal blood lymphocytes from 5 donors, using the same probe combination, this CNA pattern was not observed in any cells (< 0.2%).

In 14 of 21 cases, ≥ 1 driver CNAs were shared between diagnosis and relapse. Ig/TCR clonality data when available (see supplemental Table 6, data available on 15 patients) and conservation of *ETV6-RUNX1* fusion (as shown for UPN14, UPN15, and UPN19; supplemental Figure 8) indicated that relapses originated from within the clones present at diagnosis.

A principal and novel objective of this study was to compare SNP array–defined CNAs in relapse versus matched diagnosis samples to gain some insight into the clonal origins of late and very late relapse in *ETV6-RUNX1*$^+$ ALL. Other studies have looked at this issue in childhood ALL in general or *ETV6-RUNX1*$^+$ ALL in particular[25] and have drawn the conclusion that relapses (undefined by time from diagnosis) can emerge from either major or minor subclones present at diagnosis.[22,23,39] Distinct from previous studies we focused entirely on the subset of ALL with *ETV6-RUNX1* to ascertain whether the apparent origin from major or minor subclones was associated with time to relapse. In particular, we were interested in the biologically interesting phenomenon of very late relapse in childhood ALL. These relapses can occur intraclonally ≤ 20 years after initial diagnosis.[15,16,40] These have included *ETV6-RUNX1*$^+$ cases. A striking feature is that they are often clinically responsive rather than drug resistant, and durable second remissions and cure are possible. One possibility we and others have previously suggested was that persistent preleukemic clones harboring *ETV6-RUNX1*, the initiating lesion but no other genetic changes, might be the reservoir for such late relapses.[7,8,13,19,20,41]

Others have interpreted clonal origins of relapse in ALL in the context of a linear model of clonal evolution in ALL with minor subclones considered as ancestral to major subclones.[22,25] Recent single-cell analysis with multiple FISH probes for detecting CNAs indicates rather a complex, nonlinear, branching clonal structure.[42,43] In concordance with our previous analyses, the FISH analysis performed in patient UPN2 showed genetic diversity at both presentation and relapse. At presentation we observed a dominant clone with duplicated fusion gene and 2 copies of *CDKN2A*, alongside a minor clone with duplicated fusion and

1 copy of *CDKN2A*. At relapse this clone with loss of 1 copy of *CDKN2A* is not detectable, but "presentation cells" (duplication of fusion gene and 2 copies of *CDKN2A*) represent a minor clone next to the dominant relapse clone (duplication of fusion gene and complete loss of *CDKN2A*). The use of single-cell FISH underlines the limitations of using SNP arrays to study the genetics underlying the biology of relapse. Deductions on clonal origins of relapse on the basis of SNP array data should therefore, we suggest, be limited to the likelihood that they are derived from either the dominant or major subclone at diagnosis or from a minor subclone, irrespective of subclonal evolutionary relationships. We devised a scheme to accommodate these possibilities, defining 4 types of relapses in total (Table 4). A clear conclusion from this analysis is that, in accord with other studies, relapses can originate from either major or minor subclones present at diagnosis.

The size of the subclone at diagnosis might be anticipated to influence time to relapse, as reported in some previous studies.[39,44] However, in this series, there was no discernable relationship between early or late relapses and origins from minor or major clones at diagnosis. The basis for this discrepancy with prior data are unclear, but it might reflect particular biologic properties of the *ETV6-RUNX1*$^+$ subset of ALL or the fact that prior studies included more on-treatment, early relapses. The latter might be more likely to be drug-resistant subclones selected by treatment as evidenced by the low frequency of sustained second remissions in such cases. Off-treatment ($>3$ years after diagnosis) relapses of *ETV6-RUNX1*$^+$ ALL are usually responsive to second remission inductions, suggesting that their protracted survival after initial diagnosis and therapy was based on properties other than mutation-based drug resistance. There is some evidence that such subclones (identified by clonotypic IgH sequences) may respond slowly to induction chemotherapy.[39] One possibility is that this reflects relative quiescence and associated drug insensitivity rather than more classic, mutation-based resistance. Sustained quiescence would explain the extraordinary length of clinical remission in some of these cases. In the absence of a clear relationship between size of relapse clone at initial presentation and time to relapse in our series, we sought potential relationships between our newly devised relapse classification, number of relapse driver mutations, and overall outcome. No correlation was observed between our relapse classification, relapse drivers, and remission duration. As a consequence we cannot recommend a monitoring scheme to identify low- or high-risk relapses. We did however observe that all patients with type 4 relapses (4 of 4) remain in complete continuous remission, whereas only 5 of 15 patients with a type 1-3 relapse are alive and in continuous remission (supplemental Table 1). One possible explanation for this observation is that premalignant clones without CNAs have a more abbreviated proliferative history and, if so, will be statistically less likely to harbor drug-resistance mutations.[45]

Preleukemic clones in ALL have been detected as harboring *ETV6-RUNX1* gene fusions but no other discernable genetic alterations.[4,8] Studies with monozygotic twins with discordant ALL, neonatal blood spot scrutiny, and cord blood screening all suggest that these clones exist at a low level, $10^{-3}$ to $10^{-4}$, of B lineage cells and can persist throughout childhood.[3,5,8,46-48] We previously suggested that such preleukemic clones, perhaps as a consequence of slow growth or quiescence, might be relatively resistant to ablation by chemotherapy, would persist during and after maintenance chemotherapy, and occasionally give rise to another de novo ALL masquerading as a conventional although late off-treatment relapse.[19,20] Evidence that appeared to support this view was obtained by comparing genomic boundaries of *ETV6* deletion at relapse versus diagnosis whereby they frequently were found to be different. This indicated that the relapse emerged from a minor subclone that did not harbor the *ETV6* deletion that was present in most cells at diagnosis.[19,20] The comprehensive genetic profiles made available by high-resolution SNP arrays provide a more stringent assessment of this hypothesis. If persistent preleukemic cells (defined as *ETV6-RUNX1* fusion-only clones) do provide the source of off-treatment late or very late relapses, then clearly not only *ETV6* but *all* the specific CNAs observed at relapse should be absent at diagnosis, either at the major or minor subclone level. This would correspond to our type 4 relapses (Table 2). As described, we observed 4 such cases. Three cases relapsed between 3 and 5 years from diagnosis, and 1 case presented as a very late relapse. Of the very late relapses (5-9 years 11 months) only 1 (UPN19; supplemental Figure 3) was classified as a type 4 relapse, possibly of preleukemic clonal origin. Overall our data indicate variable but often prolonged quiescence for ALL stem cells with multiple genetic abnormalities.

## Acknowledgments

We thank patients, parents, and hospital staff for their valuable collaboration.

This work was supported by a Leukemia Research Fund (LRF) grant (M.G.), Kay Kendall Intermediate Fellowship (F.W.v.D.) and (grants MSM0021620813 and NS/1000-4; J.Z.).

## Authorship

Contribution: F.W.v.D., L.K., and M.G. designed the research; F.W.v.D. and S.H. performed the research; F.W.v.D. and M.G. analyzed the data and wrote the paper; S.C. and K.A. performed confirmatory FISH; C.B. provided helpful discussion; H.K., J.Z., C.E., and V.S. contributed patient samples; A.F. provided research supervision; and C.E. and A.F. cloned the *ETV6-RUNX1* genomic fusion gene breakpoints.

Conflict-of-interest disclosure: The authors declare no competing financial interests.

Correspondence: Mel Greaves, Section of Haemato-Oncology, Institute of Cancer Research, Brookes Lawley Bldg, 15 Cotswold Rd, Sutton, SM2 5NG, United Kingdom; e-mail: mel.greaves@icr.ac.uk.

## References

1. Harrison CJ, Moorman AV, Barber KE, et al. Interphase molecular cytogenetic screening for chromosomal abnormalities of prognostic significance in childhood acute lymphoblastic leukaemia: a UK Cancer Cytogenetics Group Study. *Br J Haematol.* 2005;129(4):520-530.
2. Jabber Al-Obaidi MS, Martineau M, Bennett CF, et al. ETV6/AML1 fusion by FISH in adult acute lymphoblastic leukemia. *Leukemia.* 2002;16(4):669-674.
3. Ford AM, Bennett CA, Price CM, Bruin MC, Van Wering ER, Greaves M. Fetal origins of the TEL-AML1 fusion gene in identical twins with leukemia. *Proc Natl Acad Sci U S A.* 1998;95(8):4584-4588.
4. Greaves MF, Wiemels J. Origins of chromosome translocations in childhood leukaemia. *Nat Rev Cancer.* 2003;3(9):639-649.
5. Wiemels JL, Ford AM, Van Wering ER, Postma A, Greaves M. Protracted and variable latency of acute lymphoblastic leukemia after TEL-AML1 gene fusion in utero. *Blood.* 1999;94(3):1057-1062.
6. Mori H, Colman SM, Xiao Z, et al. Chromosome

translocations and covert leukemic clones are generated during normal fetal development. *Proc Natl Acad Sci U S A.* 2002;99(12):8242-8247.

7. Tsuzuki S, Seto M, Greaves M, Enver T. Modeling first-hit functions of the t(12;21) TEL-AML1 translocation in mice. *Proc Natl Acad Sci U S A.* 2004; 101(22):8443-8448.
8. Hong D, Gupta R, Ancliff P, et al. Initiating and cancer-propagating cells in TEL-AML1-associated childhood leukemia. *Science.* 2008; 319(5861):336-339.
9. O'Connor HE, Butler TA, Clark R, et al. Abnormalities of the ETV6 gene occur in the majority of patients with aberrations of the short arm of chromosome 12: a combined PCR and Southern blotting analysis. *Leukemia.* 1998;12(7):1099-1106.
10. Schultz KR, Pullen DJ, Sather HN, et al. Risk- and response-based classification of childhood B-precursor acute lymphoblastic leukemia: a combined analysis of prognostic markers from the Pediatric Oncology Group (POG) and Children's Cancer Group (CCG). *Blood.* 2007;109(3): 926-935.
11. Seeger K, von Stackelberg A, Taube T, et al. Relapse of TEL-AML1–positive acute lymphoblastic leukemia in childhood: a matched-pair analysis. *J Clin Oncol.* 2001;19(13):3188-3193.
12. Harbott J, Viehmann S, Borkhardt A, Henze G, Lampert F. Incidence of TEL/AML1 fusion gene analyzed consecutively in children with acute lymphoblastic leukemia in relapse. *Blood.* 1997; 90(12):4933-4937.
13. Konrad M, Metzler M, Panzer S, et al. Late relapses evolve from slow-responding subclones in t(12;21)-positive acute lymphoblastic leukemia: evidence for the persistence of a preleukemic clone. *Blood.* 2003;101(9):3635-3640.
14. Forestier E, Heyman M, Andersen MK, et al. Outcome of ETV6/RUNX1-positive childhood acute lymphoblastic leukaemia in the NOPHO-ALL-1992 protocol: frequent late relapses but good overall survival. *Br J Haematol.* 2008;140(6):665-672.
15. Chow CD, Dalla-Pozza L, Gottlieb DJ, Hertzberg MS. Two cases of very late relapsing ALL carrying the TEL:AML1 fusion gene. *Leukemia.* 1999;13(11): 1893-1894.
16. Vora A, Frost L, Goodeve A, et al. Late relapsing childhood lymphoblastic leukemia. *Blood.* 1998; 92(7):2334-2337.
17. Chessells JM. Relapsed lymphoblastic leukaemia in children: a continuing challenge. *Br J Haematol.* 1998;102(2):423-438.
18. Lawson SE, Harrison G, Richards S, et al. The UK experience in treating relapsed childhood acute lymphoblastic leukaemia: a report on the medical research council UKALLR1 study. *Br J Haematol.* 2000;108(3):531-543.
19. Ford AM, Fasching K, Panzer-Grumayer ER, Koenig M, Haas OA, Greaves MF. Origins of "late" relapse in childhood acute lymphoblastic leukemia with TEL-AML1 fusion genes. *Blood.* 2001;98(3):558-564.
20. Zuna J, Ford AM, Peham M, et al. TEL deletion analysis supports a novel view of relapse in childhood acute lymphoblastic leukemia. *Clin Cancer Res.* 2004;10(16):5355-5360.
21. Mullighan CG, Goorha S, Radtke I, et al. Genome-wide analysis of genetic alterations in acute lymphoblastic leukaemia. *Nature.* 2007; 446(7137):758-764.
22. Mullighan CG, Phillips LA, Su X, et al. Genomic analysis of the clonal origins of relapsed acute lymphoblastic leukemia. *Science.* 2008; 322(5906):1377-1380.
23. Panzer-Grumayer ER, Cazzaniga G, van der Velden VH, et al. Immunogenotype changes prevail in relapses of young children with TEL-AML1-positive acute lymphoblastic leukemia and derive mainly from clonal selection. *Clin Cancer Res.* 2005;11(21):7720-7727.
24. Yang JJ, Bhojwani D, Yang W, et al. Genome-wide copy number profiling reveals molecular evolution from diagnosis to relapse in childhood acute lymphoblastic leukemia. *Blood.* 2008; 112(10):4178-4183.
25. Kuster L, Grausenburger R, Fuka G, et al. ETV6/RUNX1-positive relapses evolve from an ancestral clone and frequently acquire deletions of genes implicated in glucocorticoid signaling. *Blood.* 2011;117(9):2658-2667.
26. Nannya Y, Sanada M, Nakazaki K, et al. A robust algorithm for copy number detection using high-density oligonucleotide single nucleotide polymorphism genotyping arrays. *Cancer Res.* 2005; 65(14):6071-6079.
27. Li C, Wong WH. Model-based analysis of oligonucleotide arrays: expression index computation and outlier detection. *Proc Natl Acad Sci U S A.* 2001;98(1):31-36.
28. Lin M, Wei LJ, Sellers WR, Lieberfarb M, Wong WH, Li C. dChipSNP: significance curve and clustering of SNP-array-based loss-of-heterozygosity data. *Bioinformatics.* 2004;20(8): 1233-1240.
29. Buckle VJ, Rack K. Fluorescent in situ hybridisation. In: Davies KE, ed. *Human Genetic Analysis.* Oxford, United Kingdom: IRL Press; 1993:59-82.
30. von Goessel H, Jacobs U, Semper S, et al. Cluster analysis of genomic ETV6-RUNX1 (TEL-AML1) fusion sites in childhood acute lymphoblastic leukemia. *Leuk Res.* 2009;33(8):1082-1088.
31. Kawamata N, Ogawa S, Seeger K, et al. Molecular allelokaryotyping of relapsed pediatric acute lymphoblastic leukemia. *Int J Oncol.* 2009;34(6): 1603-1612.
32. Kawamata N, Ogawa S, Zimmermann M, et al. Molecular allelokaryotyping of pediatric acute lymphoblastic leukemias by high-resolution single nucleotide polymorphism oligonucleotide genomic microarray. *Blood.* 2008;111(2):776-784.
33. Kuiper RP, Schoenmakers EF, van Reijmersdal SV, et al. High-resolution genomic profiling of childhood ALL reveals novel recurrent genetic lesions affecting pathways involved in lymphocyte differentiation and cell cycle progression. *Leukemia.* 2007;21(6):1258-1266.
34. Lilljebjorn H, Soneson C, Andersson A, et al. The correlation pattern of acquired copy number changes in 164 ETV6/RUNX1-positive childhood acute lymphoblastic leukemias. *Hum Mol Genet.* 2010;19(16):3150-3158.
35. Huppi K, Volfovsky N, Runfola T, et al. The identification of microRNAs in a genomically unstable region of human chromosome 8q24. *Mol Cancer Res.* 2008;6(2):212-221.
36. Schiffman JD, Hodgson JG, VandenBerg SR, et al. Oncogenic BRAF mutation with CDKN2A inactivation is characteristic of a subset of pediatric malignant astrocytomas. *Cancer Res.* 2010; 70(2):512-519.
37. Guan Y, Kuo WL, Stilwell JL, et al. Amplification of PVT1 contributes to the pathophysiology of ovarian and breast cancer. *Clin Cancer Res.* 2007; 13(19):5745-5755.
38. Storlazzi CT, Fioretos T, Paulsson K, et al. Identification of a commonly amplified 4.3 Mb region with overexpression of C8FW, but not MYC in MYC-containing double minutes in myeloid malignancies. *Hum Mol Genet.* 2004;13(14):1479-1485.
39. Choi S, Henderson MJ, Kwan E, et al. Relapse in children with acute lymphoblastic leukemia involving selection of a preexisting drug-resistant subclone. *Blood.* 2007;110(2):632-639.
40. Ly-Sunnaram B, Henry C, Gandemer V, et al. Late ovarian relapse of TEL/AML1 positive ALL confirming that TEL deletion is a secondary event in leukemogenesis. *Leuk Res.* 2005;29(9):1089-1094.
41. Sabaawy HE, Azuma M, Embree LJ, Tsai HJ, Starost MF, Hickstein DD. TEL-AML1 transgenic zebrafish model of precursor B cell acute lymphoblastic leukemia. *Proc Natl Acad Sci U S A.* 2006; 103(41):15166-15171.
42. Anderson K, Lutz C, van Delft FW, et al. Genetic variegation of clonal architecture and propagating cells in leukaemia. *Nature.* 2011;469(7330):356-361.
43. Greaves M. Darwin and evolutionary tales in leukemia. The Ham-Wasserman Lecture. *Hematology Am Soc Hematol Educ Program.* 2009;3-12.
44. Henderson MJ, Choi S, Beesley AH, et al. Mechanism of relapse in pediatric acute lymphoblastic leukemia. *Cell Cycle.* 2008;7(10):1315-1320.
45. Komarova NL, Wodarz D. Drug resistance in cancer: principles of emergence and prevention. *Proc Natl Acad Sci U S A.* 2005;102(27):9714-9719.
46. Greaves MF, Maia AT, Wiemels JL, Ford AM. Leukemia in twins: lessons in natural history. *Blood.* 2003;102(7):2321-2333.
47. Maia AT, Ford AM, Jalali GR, et al. Molecular tracking of leukemogenesis in a triplet pregnancy. *Blood.* 2001;98(2):478-482.
48. Gale KB, Ford AM, Repp R, et al. Backtracking leukemia to birth: identification of clonotypic gene fusion sequences in neonatal blood spots. *Proc Natl Acad Sci U S A.* 1997;94(25):13950-13954.